Computer Communications 33 (2010) 852–859

Contents lists available at ScienceDirect

Computer Communications

journal homepage: www.elsevier.com/locate/comcom

# Admission region of triple-play services in wireless home networks

Fengdan Wan, Lin Cai, Emad Shihab, Aaron Gulliver *

*Department of Electrical & Computer Engineering, University of Victoria, P.O. Box 3055, STN CSC Victoria, BC, Canada V8W 3P6*

ARTICLE INFO

*Article history:*
Received 13 August 2008
Received in revised form 14 October 2009
Accepted 15 December 2009
Available online 4 January 2010

*Keywords:*
IPTV
Quality of service (QoS)
CBQ
Fluid model

ABSTRACT

A heterogeneous wired and wireless network architecture is considered for home networks to support Internet Protocol TV (IPTV), voice, and data, the so-called triple-play services. To satisfy the quality of service (QoS) requirements for different traffic classes, class-based queueing (CBQ) is deployed at home gateways and routers. To estimate the network capacity and decide on an appropriate resource management scheme, we develop an analytical framework to quantify the maximum number of IPTV connections that can be supported with guaranteed QoS over wired and multi-hop wireless networks. We extend the fluid-flow model to capture both the burstiness of IPTV sources and the time-varying characteristics of multi-hop wireless paths. Heterogeneous traffic and CBQ are considered in the model. Simulation results over wired and multi-hop wireless paths are given which validate the analysis. The results presented provide important guidelines for the planning of future home networks for triple-play services. They also provide important insights into how to efficiently support heterogeneous traffic with stringent QoS requirements over wireless and wired networks.



## 1. Introduction

Internet Protocol TV (IPTV) has been predicted to be a major technology winner. Telecommunication service providers are racing to deliver IPTV/Video on Demand (VoD), voice, and data, the so-called triple-play services. One of the major challenges in rolling out these new services is to satisfy the quality of service (QoS) requirements of heterogeneous applications simultaneously inside the home. These challenges are quite different from those faced in traditional home networks, where only data applications are considered. How to design and develop last-meter broadband home networks so consumers can enjoy triple-play services anytime, in any room, without rewiring their homes is a critical issue that needs to be addressed. This is key to the success of IPTV.

Because of the complimentary characteristics and disparities of wired and wireless communication technologies, the architecture of future broadband home networks is anticipated to be a heterogeneous wireless and wired network. Existing wired links will create the backbone of home networks, providing reliable, high data rate communications. Emerging high data rate wireless technologies will then deliver the traffic to the entire home ubiquitously, through single-hop or multiple-hop paths.

How to efficiently utilize limited network resources to provide triple-play services with guaranteed QoS is a challenging problem. Due to the heterogeneous characteristics and different QoS requirements of IPTV, data and voice traffic, we propose to deploy class-based queueing (CBQ) in-home routers. CBQ only comes into effect when congestion occurs. It protects each traffic class from the others, according to the portion of bandwidth reserved for each class.

Given the home network architecture, link sharing mechanism, and the throughput of wired and wireless links, an immediate question is how many IPTV, data and voice connections can be supported simultaneously with guaranteed QoS. In other words, what is the admission region of triple-play traffic in a home network? Because of the highly variable data rates and stringent QoS requirements of IPTV traffic, to answer this question, a quantitative analysis of queue behavior with multiplexed video, data and voice over both wireless and wired links is necessary. This not only helps service providers and consumers to choose the best distribution technologies, but also provides important guidelines for planning future home networks.

The fluid-flow model analysis of queue performance was first investigated in [13]. This model was extended in [14] to analyze the buffer behavior with multiple sources and multiple servers. The model in [14] was used in [15] for the case of a single-hop On–Off wireless channel. Different from the existing work, we consider a finite state wireless channel with variable data rates, which yields a more accurate representation for high data rate wireless systems. In [16], we evaluated IPTV performance over wired and wireless networks. To ensure QoS for heterogeneous traffic, separate queues for two traffic classes were used in [17], where a low priority class can consume residual bandwidth only when a high priority class is not able to consume the entire link bandwidth. This

* Corresponding author. Tel.: +1 250 721 6028; fax: +1 250 721 6052.
*E-mail addresses:* fdwan@ece.uvic.ca (F. Wan), cai@ece.uvic.ca (L. Cai), emads@ece.uvic.ca (E. Shihab), agullive@ece.uvic.ca (A. Gulliver).

0140-3664/$ - see front matter © 2009 Elsevier B.V. All rights reserved.
doi:10.1016/j.comcom.2009.12.006

can be seen as a special case of CBQ. The general CBQ behavior over a heterogeneous combined wired and wireless network has not been investigated.

The main contributions of this paper are threefold. We first propose a wireless and wired mesh network architecture for in-home triple-play distribution. Second, we develop an analytical framework for quantifying the admission region of home networks, considering the traffic and communication link characteristics, with and without CBQ. This can be used to investigate the relationship between system parameters. The analytical framework is also applicable to other networks. In addition, extensive simulations using H.264 video traces have been conducted to validate our analysis.

The remainder of the paper is organized as follows. We introduce the network architecture and system model in Section 2. The fluid model analysis to quantify the admission region in wireless and wired networks is given in Section 3, followed by simulation and numerical results in Section 4. Section 5 presents some concluding remarks.

## 2. System model

### 2.1. Network architecture and video codec

To support triple-play services anytime, in any room, without rewiring existing houses, we propose a wireless and wired network architecture for in-home traffic distribution, as shown in Fig. 1. Existing wired links, like coaxial cables, phone lines, and powerlines compose the network backbone. Wireless access points (APs) further relay the IPTV traffic to any corner of the home via single or multiple hops, using high data rate wireless communication technologies such as IEEE 802.11n, Ultra-Wide Band (UWB), millimeter wave (mmWave), etc.

Although IEEE 802.11-based wireless access technologies have been widely deployed, the lack of QoS support makes them undesirable for supporting IPTV. In the wireless domain, we thus adopt the architecture and MAC protocol specified in the IEEE 802.15.3 standard for our system model, as it has been developed for wireless personal area networks (WPANs) supporting high data rate multimedia applications. A WPAN is suitable for indoor wireless networks, with its short range, high capacity and low interference properties. In an IEEE 802.15.3 WPAN, several devices can autonomously form a piconet, with one device selected as the piconet coordinator (PNC). The PNC can collect global information about the piconet and allocate radio resources or schedule channel times to all devices in the piconet according to their requests. All devices can communicate in a peer-to-peer fashion using the allocated channel times. Since the PNC is selected first, the MAC protocol adopted in our model is the centralized controller. Hidden or exposed nodes and link layer contention problems are negligible. In the standard, as shown in Fig. 2, time is slotted in a superframe structure where each superframe consists of a beacon period (BP), a contention access period (CAP) using CSMA/CA as the access protocol, and a contention-free period named channel time allocation period (CTAP) using Time Division Multiple Access (TDMA). All devices can request channel time through contention in the CAP, and use the allocated time in the CTAP for transmission. If the traffic must be relayed with multiple hops, the PNC should allocate separate time slots for each hop.

For IPTV video sources, advanced source coding technologies have been developed to aggressively increase the compression ratio and reduce the source data rate. MPEG-4/H.264 has about twice the compression efficiency of MPEG-2, so it is anticipated to be widely employed for high definition (HD) content. For this reason, we consider MPEG-4/H.264 video sources in our system.

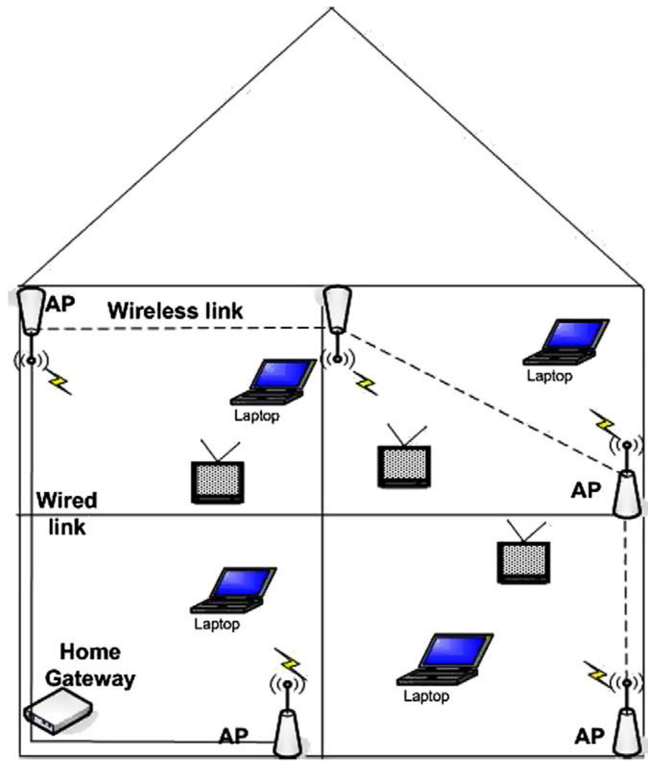


**Fig. 1.** Home network architecture.

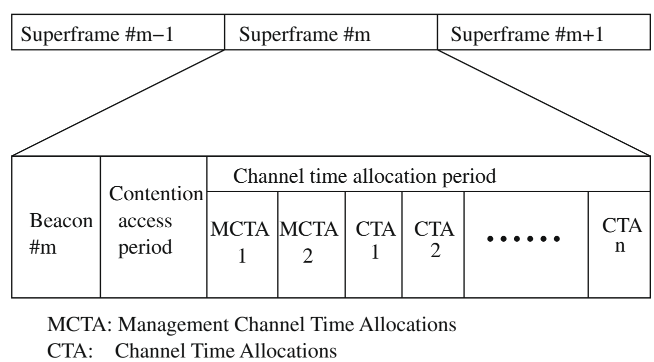


**Fig. 2.** Superframe structure defined in the IEEE 802.15.3 MAC protocol.

### 2.2. Class-based queuing management

With the existence of heterogeneous traffic, to accurately obtain the admission region of triple-play services in a wired or wireless bottleneck path, the traffic characteristics and QoS constraints of supported applications need to be considered. Data traffic is more bursty in nature, and IPTV traffic has very stringent delay and loss requirements. Thus, we propose to deploy a class-based resource management scheme before the home gateway and APs. CBQ is a link-sharing approach which enables the gateway to distribute bandwidth on local links in response to local needs [1].

The data packets and video packets are classified into two classes.[1] In the absence of congestion, a general scheduler, first in first

[1] Voice traffic can be represented as another separate class. However, since the volume of voice traffic is much smaller than that of video or data traffic, its impact on the admission region of IPTV connections is negligible, and therefore is ignored in this paper.

out (FIFO) or round-robin scheduler, could be used. When congestion occurs (when one or both classes require more than their allocated bandwidth), CBQ invokes a link-sharing scheduler to rate-limit the over-limit class(es) to their assigned capacity. In this way, CBQ can prevent starvation of data traffic and ensure the QoS requirements of IPTV traffic are met. According to CBQ, the available capacity in the output link for the two classes can be denoted as

$$C_v(t) = \max\{C - \lambda_d(t), (1-p)C\},$$
$$C_d(t) = \max\{C - \lambda_v(t), pC\}, \quad (1)$$

where the arrival rates of IPTV and data traffic are $\lambda_v$ and $\lambda_d$, respectively, and $C$ is the bottleneck link capacity. The instantaneous output rate of each class is bounded by the available bandwidth at any time instant. Note that different from the Generalized Processor Sharing (GPS) approach (e.g., weighted fair queue), that guarantees the long-term average bandwidth received by different classes, the CBQ scheme adopted here guarantees that each traffic class receives its allocated bandwidth over the relevant time interval [1]. Thus, it can protect IPTV traffic from bursty data traffic. Even if the data traffic is idle for a long period, it cannot occupy more instantaneous bandwidth as compensation (which is not true using GPS), so the instantaneous bandwidth allocated to IPTV traffic is guaranteed. On the other hand, if any traffic class is idle, the other classes can occupy the total link bandwidth to achieve multiplexing gain.

Not needing to track the history of on-going flows, CBQ is much simpler to implement than GPS-based schedulers. The different class queues are *virtual* queues for implementation. All packets are multiplexed into one queue with the condition that a certain portion of the data packets is inserted in between video packets. This portion is set according to the link-sharing parameter and the size of the video and data packets. Thus, CBQ can easily be implemented in practice.

### 2.3. Wireless channel model

In the wireless domain, advanced wireless technologies can adapt the data rate according to the channel conditions (which are typically time-varying). For instance, the over-the-air data rate of IEEE 802.11n varies from 200 Mbps to 540 Mbps, and that of UWB varies from 53.3 Mbps to 480 Mbps, or even higher. With physical layer adaptive rate control and link layer retransmissions, from an upper layer protocol perspective, packet losses due to transmission errors are negligible. However, the link throughput (or data rate) observed by the upper layer protocols is time-varying. We choose a finite state Markov model as the packet-level wireless channel model, because it is recognized to be reasonably accurate in capturing wireless channel variations [18].

With this model, each state corresponds to a different average signal-to-noise ratio (SNR) and thus a different data rate. The state-transition probabilities are chosen to reflect the time-correlation of the wireless channel. Fig. 3 depicts a three-state Markov chain wireless channel model.

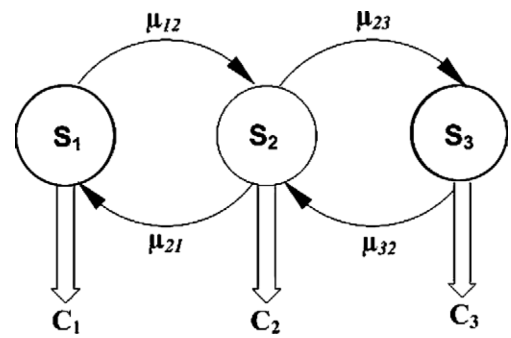


**Fig. 3.** Three-state wireless channel model.

### 2.4. Fluid-flow model of video traffic with constant service rate

Inside the home, all IPTV downstream traffic is delivered from the home gateway to set-top boxes or other devices. All transmissions in the wired network using a wired technology (such as coaxial cable, powerline, or phoneline) are in the same collision domain, and thus share the wired link bandwidth which is assumed constant. For video transmissions over constant data rate links, the well known fluid-flow model can be applied. In [2], a variable bit rate video source is modeled as the multiplexing of 20 mini sources. Each mini source independently alternates between an "off" state and an "on" state, and $A$ bps are generated during the "on" state. The average residence times in the "off" state and "on" state are $1/\alpha$ and $1/\beta$ seconds, respectively. Since H.264 has a higher compression ratio than the source codes considered in [2], we use fewer mini sources to emulate the more bursty video sources. Our experimental results suggest that using eight mini sources to model one H.264 video source is appropriate.

Let $F_i(x)$ denote the probability that the queue length is less than $x$, given that $i$ mini sources are on. With a constant service rate of $C$ bps and $M$ mini sources in total, the equilibrium queue length distribution at the home gateway is subject to [2]

$$\frac{d\mathbf{F}(x)}{dx}\mathbf{D} = \mathbf{F}(x)\mathbf{B}, \quad (2)$$

where $\mathbf{D}$ is an $(M+1)\times(M+1)$ diagonal matrix

$$\mathbf{D} = \mathbf{R}_s - C\mathbf{I},$$

and $\mathbf{F}(x)$ is the row vector $[F_0(x)\ F_1(x)\ \cdots\ F_N(x)]$, $\mathbf{R}_s = \mathrm{diag}\{0, 1, \ldots, M \times A\}$. The underlying continuous time Markov chain of the video source model is represented by the generating matrix

$$\mathbf{B}_s = \begin{pmatrix} -M\alpha & M\alpha & 0 & \cdots \\ \beta & -(M-1)\alpha-\beta & (M-1)\alpha & \cdots \\ \vdots & \vdots & \vdots & \vdots \\ 0 & \cdots & \cdots & -M\beta \end{pmatrix}.$$

Given the fluid model, we can obtain the cumulative distribution function (CDF) of the queue length as

$$F(x) = 1 + \sum_{i:Re[z_i<0]} a_i \sum_{j=1}^{M} \phi_{ij} \exp(z_i x),$$

where $z_i$ and $\mathbf{\Phi}_i$ are the negative left eigenvalues and the corresponding eigenvectors of the matrix $\mathbf{B}_s\mathbf{D}^{-1}$

$$z_i\mathbf{\Phi}_i\mathbf{D} = \mathbf{\Phi}_i\mathbf{B}_s. \quad (3)$$

The coefficients $a_i$ can be obtained from the boundary conditions, i.e., $F_j(0) = 0$ for $j > C/A$.

The survivor function $G(x)$, which represents the probability of buffer overflow, is the complementary distribution of $F(x)$

$$G(x) = 1 - F(x) = -\sum_{i:Re[z_i<0]} a_i \sum_{j=1}^{M} \phi_{ij} \exp(z_i x). \quad (4)$$

In summary, given $\mathbf{B}$, the generating matrix of the underlying Markov process representing the variation of effective bandwidth, and $\mathbf{D}$ for the arrival rate, the queue length distribution can be obtained. Then by using (4), the probability of buffer overflow can be predicted.

Given the QoS requirements of IPTV traffic, including the loss rate and delay bound, we can limit the number of connections and choose an appropriate buffer size. For instance, given the delay bound in a home network, we can determine the required queue length and thus the buffer size so the packet delay will not exceed the delay bound. From (4), we can determine the maximum number of connections that can be supported with a guaranteed loss rate due to buffer overflow.

## 3. Fluid model analysis framework for triple-play traffic over wireless networks

To quantify the admission region of IPTV traffic with the existence of data traffic, and identify the bottleneck in the heterogeneous wired and wireless mesh home network, the fluid model is extended to consider a time-varying single-hop wireless link with a variable data rate. This is later extended to multi-hop wireless paths. We study the queue behavior and admission region for homogeneous IPTV traffic first, and then consider heterogeneous traffic, with and without CBQ.

### 3.1. IPTV over a single-hop wireless channel

For the wireless link, a finite state Markov chain is used to model the time-varying service rates. Let $C_j$ denote the data rate (service rate of the wireless link) in state $j$, and assume that the total number of states of the wireless link is $N$. We then have $\mathbf{C} = \mathrm{diag}\{C_1, C_2, \ldots, C_N\}$. The generating matrix of the underlying continuous time Markov process $\mathbf{B_c}$ is defined by

$$\mathbf{B_c} = \begin{pmatrix} \mu_{11} & \mu_{12} & \cdots & \mu_{1N} \\ \mu_{21} & \mu_{22} & \cdots & \mu_{2N} \\ \vdots & \vdots & \vdots & \vdots \\ \mu_{N1} & \mu_{N2} & \cdots & \mu_{NN} \end{pmatrix},$$

where $\mu_{kj}$, $1 \leqslant k, j \leqslant N$ is the state transition probability from state $k$ to state $j$, and $\mu_{kk} = -\sum_{j=1 j\neq k}^{N} \mu_{kj}$.

Let $F_{i,j}(t,x)$ be the probability that the queue length at the wireless AP does not exceed $x$ at time $t$, when the wireless link is in state $j$ and $i$ mini sources are on. The probability of one source turning on or turning off during a small time interval $\Delta t$ is $\alpha\Delta t$ or $\beta\Delta t$, respectively. Similar to [13], we can show that the queue distribution in equilibrium, which is obtained when $\Delta t \to 0$ and $\partial F_{i,j}/\partial t = 0$, satisfies

$$(iA - C_j)\frac{dF_{i,j}(x)}{dx} = \sum_{k=1}^{N}[N-(i-1)]\alpha\Delta t F_{i-1,k}\mu_{kj} + \sum_{k=1}^{N}(i+1) \times \beta\Delta t F_{i+1,k}\mu_{kj} + \sum_{k=1}^{N}[(M-i)\alpha + i\beta]F_{i,k}\mu_{kj}. \quad (5)$$

Let the coupled source and link system state $s = (i,j)$ be ordered lexicographically

$$(0,1)(0,2)\cdots(0,N)\cdots(M,N).$$

A component of $\mathbf{F}$, $F_k$, denotes the CDF of the queue distribution when the system is in state $k$, $k = N(i-1)+j$ for $1 \leqslant k \leqslant N(M+1)$. In matrix notation, (5) can be written as

$$\frac{d\mathbf{F}(x)}{dx}\mathbf{D} = \mathbf{F}(x)\mathbf{B}, \quad (6)$$

which has the same structure as (2), where

$$\mathbf{B} = \mathbf{B_s} \oplus \mathbf{B_c} \triangleq \mathbf{B_s} \otimes \mathbf{I_N} + \mathbf{I_{M+1}} \otimes \mathbf{B_c}. \quad (7)$$

Here, $\oplus$ and $\otimes$ are the Kronecker sum and Kronecker product [3], respectively. In (7), $\mathbf{I_N}$ is an $N \times N$ identity matrix, thus $\mathbf{B}$ is a matrix with dimension $N(M+1)$. $\mathbf{D}$ is the $N(M+1)$ diagonal matrix

$$\mathbf{D} = \mathbf{R_s} \oplus [-\mathbf{C}]. \quad (8)$$

Given $\mathbf{B}$ and $\mathbf{D}$, the probability of buffer overflow can be obtained by solving (6).

The effective capacity reflects the *stochastic bounded capacity* for a (or a number of) traffic source(s) accessing the buffer, conditioned on the loss probability $P_L$ and the maximum buffer size $x$. High variance input traffic has a higher effective capacity, which leads to fewer connections accommodated by a link. On the other hand, with highly variant output links, the effective capacity will decrease, which also results in fewer admitted connections. The results in Section 4 also demonstrate this tendency.

### 3.2. IPTV over a multi-hop wireless path

To deliver IPTV traffic from a home gateway to anywhere inside or even outside the home via power constrained wireless technologies with a limited transmission range (e.g., UWB), multi-hop wireless relays may be needed. In this section, the fluid model is further extended to multi-hop wireless paths.

Assume that the indoor multi-hop wireless path consists of $k$ hops. These $k$ hops are within the interference range of each other, so they cannot transmit simultaneously. This is a reasonable assumption for a home networking environment. Since different hops require separate channel times in IEEE 802.15.3 CTAPs, the transmission rate of a packet over a $k$-hop path is

$$C = \left[\sum_{m=1}^{k} 1 \Big/ C_m\right]^{-1}, \quad (9)$$

where $C_m$ is the link service rate of the $m$th hop.

In the following, we use a 3-hop wireless path as an example, but the approach can be applied to any number of hops. Let $\mathbf{B_c^{(1)}}$, $\mathbf{B_c^{(2)}}$ and $\mathbf{B_c^{(3)}}$ be the generating matrices for the underlying continuous time Markov chains of the first, second and third hops, respectively. If each hop has three states corresponding to three different service rates, as shown in Fig. 3, each of these would be a $3 \times 3$ matrix with components represented by $\mu_{ij}$, $1 \leqslant i \leqslant 3$, $1 \leqslant l \leqslant 3$. Let the state of the multi-hop path be ordered lexicographically. Thus, the generating matrix for the 3-hop path, $\mathbf{B_c}$, has dimension 27

$$\mathbf{B_c} = \mathbf{B_c^{(1)}} \oplus \mathbf{B_c^{(2)}} \oplus \mathbf{B_c^{(3)}}.$$

In each state, the corresponding service rate can be obtained from (9). The diagonal matrix $D$ is obtained from (8). $\mathbf{C}$ has dimension 27 and $C_i$ is the end-to-end data rate of the 3-hop path for state $i$.

After obtaining $\mathbf{B}$ and $\mathbf{D}$ according to (3), with (4), the probability of buffer overflow in the multi-hop case, $G(x)$, can be obtained. Thus, given the QoS requirements of IPTV traffic, the admission region and buffer size for the multi-hop path can be derived.

### 3.3. Multiplexed heterogeneous traffic in-home networks

In addition to IPTV, home networks also accommodate other applications, such as data and voice. For the queue system, the previous subsections have considered variations of the output process (transmission links). Here we further consider heterogeneous input traffic, and extend the fluid-flow analytical framework to consider heterogeneous traffic with and without CBQ.

(1) *Without CBQ:* First, we assume that all input traffic sources are independent and multiplexed into a single queue. The burstiness of the data traffic and the regularity of the voice traffic can be modeled by an irreducible, reversible Markov process [4,5]. Denote $\mathbf{B_s^{(k)}}$, $0 \leqslant k \leqslant K$, as the infinitesimal generator matrix for the underlying Markov process of the $k$th source with $N^{(k)}$ states. Then, the generating matrix representing the combination of input traffic can be obtained by

$$\mathbf{B_s} = \mathbf{B_s^{(1)}} \oplus \mathbf{B_s^{(2)}} \cdots \oplus \mathbf{B_s^{(K)}}, \tag{10}$$

where the indices of $\mathbf{B_s}$ are ordered lexicographically. The traffic arrival rate $\mathbf{R_s}$ is composed of the superposition of arrival rates for each traffic source

$$\mathbf{R_s} = \mathbf{R_s^{(1)}} \oplus \mathbf{R_s^{(2)}} \cdots \oplus \mathbf{R_s^{(K)}}. \tag{11}$$

Then the diagonal matrix can be represented as $\mathbf{D} = \mathbf{R_s} - C\mathbf{I}$ where $C$ is the constant link service rate.

If the output link is a time-varying single-hop (or multi-hop) wireless link, $\mathbf{B_c}$ is the corresponding generating matrix. Matrix $\mathbf{B}$ can then be represented as

$$\mathbf{B} = \mathbf{B_s} \oplus \mathbf{B_c} = \mathbf{B_s^{(1)}} \oplus \mathbf{B_s^{(2)}} \cdots \oplus \mathbf{B_s^{(K)}} \oplus \mathbf{B_c}, \tag{12}$$

which is obtained by substituting (10) into (7). $\mathbf{D}$ is given by (8). Here, $\mathbf{R_s}$ should be calculated using (11). A similar substitution is needed when the heterogeneous traffic is relayed by multi-hop wireless networks. Once we obtain $\mathbf{B}$ and $\mathbf{D}$, the probability of buffer overflow can be obtained when heterogeneous traffic is multiplexed.

*Remarks:* To obtain the buffer overflow probability of heterogeneous traffic multiplexed into constant capacity wired links, time-varying single-hop links, or multi-hop wireless links, a similar approach is used. The key is to obtain the generating matrix of the *aggregated* system, and derive $\mathbf{B}$ and $\mathbf{D}$ accordingly. Variations in the traffic rate and channel bandwidth have opposite effects on the admission region. The input rate of the data traffic, for example, from the IPTV traffic point of view, can be considered as a deduction from the available capacity of the output link. In addition, variations in the channel service rate (a deduction from the maximum channel capacity), can be seen as a variable input data rate. This observation matches the theory of effective capacity [6] discussed in Section 3.1.

(2) *With CBQ:* To guarantee the stringent QoS requirements of IPTV, while at the same time protecting data traffic from starvation, CBQ is employed. There are two virtual queues in the system: one for IPTV traffic and another to accommodate data traffic. Each traffic class can only consume its assigned bandwidth if the other virtual queue is not empty; otherwise, it can use all of the available link bandwidth. Assume that a fraction $(1-p)$ of the service rate is assigned to IPTV traffic and the remainder $p$ is assigned to data traffic when both queues are not empty.[2]

Denote the queue occupancy of video and data as $F_v$ and $F_d$, respectively. The evolution equations of $F_v$ and $F_d$ are

$$\begin{aligned}\frac{dF_v}{dt} &= \gamma^{(v)}(s_v) + pC - C \qquad F_d > 0,\\ &= \gamma^{(v)}(s_v) + \gamma^{(d)}(s_d) - C \qquad F_d = 0,\\ \frac{dF_d}{dt} &= \gamma^{(d)}(s_d) + (1-p)C - C \qquad F_v > 0,\\ &= \gamma^{(d)}(s_d) + \gamma^{(v)}(s_v) - C \qquad F_v = 0,\end{aligned} \tag{13}$$

where the arrival rates of video and data are $\gamma^{(v)}(s_v)$ and $\gamma^{(d)}(s_d)$, respectively. $\mathbf{S} = (s_v, s_d)$ denotes the combined system state. The queue distribution derivations for video and data are similar. We take the video queue as an example.

The equilibrium distribution of the queue for video should satisfy

$$\frac{d\mathbf{F}(x)}{dx}\mathbf{D_v} = \mathbf{F}(x)\mathbf{B_v},$$

where $\mathbf{B_v}$ represents the transition rate among states in the combined system

$$\mathbf{B_v} = \mathbf{B_s^{(v)}} \oplus \mathbf{B_s^{(d)}},$$

where $\mathbf{B_s^{(v)}}$ and $\mathbf{B_s^{(d)}}$ are the generating matrices of the underlying Markov chain for video and data traffic, respectively. Although $\mathbf{B_s^{d}}$ and $\mathbf{B_s^{v}}$ may be equivalent for the video and data queues, $\mathbf{D_d}$ and $\mathbf{D_v}$ are different. $\mathbf{D_v}$ is obtained as

$$\mathbf{D_v} = \mathbf{R_s} - C\mathbf{I} = \mathbf{R_v} \oplus \mathbf{R_{d'}} \oplus \mathbf{R_c} - C\mathbf{I}, \tag{14}$$

where $\mathbf{R_v}$ is the video arrival rate $\gamma^{(v)}(s^{(v)})$. When the arrival rate of the data traffic $\gamma^{(d)}(s_d)$ is larger than its assigned bandwidth $pC$, the link-sharing scheduler in CBQ will limit the data traffic to its assigned bandwidth. Thus, at those states $\mathbf{S} = (s_v, s_d)$ with $\gamma^{(d)}(s_d) > pC$, the arrival rate of the data is $pC$ instead of $\gamma^{(d)}(s_d)$ from the video traffic's point of view. $\mathbf{R_{d'}} = \min\left(pC, \gamma^{(d)}(s_d)\right)$ is the arrival rate for video. The coefficients $a_i$ can be obtained from the boundary conditions, i.e., $F_o(0) = 0$ for $R(\mathbf{S}) > C$. Finally, we can obtain the packet loss ratio of the video packets.

From (13), buffer overflow can only occur in those states where $F_v > 0$ (when the overall traffic arrival rate is greater than the total service rate). In equilibrium, when the queue is not filling, the probability of queue overflow is 0, so $F_v = 0$. The combined Markov process can be separated into two *virtual* states: $\Omega_o$ with $F_v > 0$ and $\Omega_u$ with $F_v = 0$. Then we have

$$\Pr(F_v \geqslant x) = \Pr(F_v \geqslant x|\Omega_o)\Pr(\Omega_o).$$

In state $\Omega_o$, $F_v$ is filling and video uses all its reserved bandwidth. Overflow only happens in those states where the total arrival rate is larger than the total capacity. In this case, congestion will occur and CBQ will limit the over-limit traffic to its allocated bandwidth.

Given the tolerable loss rates of arriving traffic, we can determine the admission region of IPTV services. At the same time, we can appropriately apportion bandwidth for IPTV and data traffic. For the multi-hop wireless case, we use the same approach and obtain $B$ and $D$ according to (12) and (8).

## 4. Performance evaluation by simulation

### 4.1. Simulation parameters

To verify the analytical results, extensive simulations have been performed using the network simulator NS-2 [7]. The home network we considered is composed of the wired backbone network and 3-hop wireless network, as shown in Fig. 1. The wired backbone can be an existing coaxial cable, phone line or power line inside the house, while the 3-hop wireless network accommodates the IEEE 802.15.3 standard. When the triple-service traffic first arrives at the home gateway, it is first carried by the wired backbone to each access point, then delivered to TV set-top boxes, computers, mobile devices, etc., via the wireless network. The overall home network performance is restricted by the bottleneck, which can be the wired network or the wireless network. The simulation results for both scenarios verify the analytical framework, and provide insight for future home network planning and as to which parameters have the greatest impact on network performance.

The H.264 video trace entitled "From Mars to China" in HDTV format (1920 × 1080) is used [8]. The average bit rate of the video is 4.85 Mbps, the variance is $3.6375 \times 10^{10}$ (bps)$^2$, the autocorrelation decay coefficient is 0.215 bps and the frame rate is 30 frames/s. In our simulations, the target is to provide up to 5 Mbps Internet data service. 5 Mbps CBR data traffic and bursty On–Off data traffic with a peak rate of 5 Mbps are investigated. For the On–Off data source, the Off period is 10 times the On period. The average On period is set to 55.605 s [9]. For simplicity, both video and data traffic are encapsulated in 1000 byte UDP packets.

For IEEE 802.15.3 [10] wireless networks, the data rate of each wireless link follows a three-state Markov chain. The payload data

[2] Although we are assuming two classes of traffic, the analysis presented here can easily be extended to any number of classes.

rate is obtained by considering the physical layer data rate and the protocol overheads. The payload transmission time, $T_{pay}$ equals $\frac{payload}{R_i}$, and $R_i$ can be 55 Mbps, 110 Mbps, or 200 Mbps, depending on the current channel state. The time to transmit a frame is

$$T_{frame} = T_a + \left(\frac{payload + RUI_h}{R_i}\right) + \left(\frac{PHY_h + MAC_h + HCS + FCS}{R_1}\right),$$

where $T_a$, $RUI_h$, $PHY_h$, $MAC_h$, $HCS$ and $FCS$ are the preamble time, RTP/UDP/IP headers, PHY header, MAC header, Header Check Sequence and Frame Check Sequence, respectively. The PHY/MAC overhead is transmitted at a base data rate of $R_1 = 55$ Mbps. The achievable throughput for the payload is then

$$C_i = \frac{T_{pay} R_i}{T_{frame} + T_g + T_{ACK} + 2SIFS},$$

where the guard time $T_g$, the ACK time $T_{ACK}$, the SIFS time and all other overhead takes the same values as in [11]. This leads to service rates of $C_1 = 40.3$ Mbps, $C_2 = 64.0$ Mbps and $C_3 = 88.7$ Mbps in states $s_1$, $s_2$ and $s_3$, respectively.

The state transition rates (per second) of the wireless link are given in the matrix $\mathbf{B_c}$ below, where $\mu_{ij}$ in the $i$th row and $j$th column is the transition rate from state $i$ to state $j$

$$\mathbf{B_c} = \begin{pmatrix} -18 & 18 & 0 \\ 2 & -16 & 14 \\ 0 & 2 & -2 \end{pmatrix}.$$

CBQ is implemented at each router. We repeat the simulations with different random seeds and each simulation runs for half an hour. The simulation results presented are the averages of 20 runs.

In Figs. 4–7, the horizontal axis denotes the total buffer for both video and data traffic. The buffer size is chosen such that the virtual buffer size for video ranges from 400 packets to 1100 packets, where the data buffer size is the closest integer value of $(1/p - 1)$ times the video buffer size.

### 4.2. Numerical and simulation results

#### 4.2.1. Wired backbone network

With a wired backbone link bandwidth of 85 Mbps, Figs. 4 and 5 show the analytical and simulation results for buffer overflow probability vs. buffer size, with a CBR data source and an On–Off data source, respectively. For the CBQ, 5% of the link bandwidth is reserved for data, and the remaining bandwidth is used to support IPTV traffic. The results show that there is a discrepancy between the analysis and simulation when the buffer size is small.

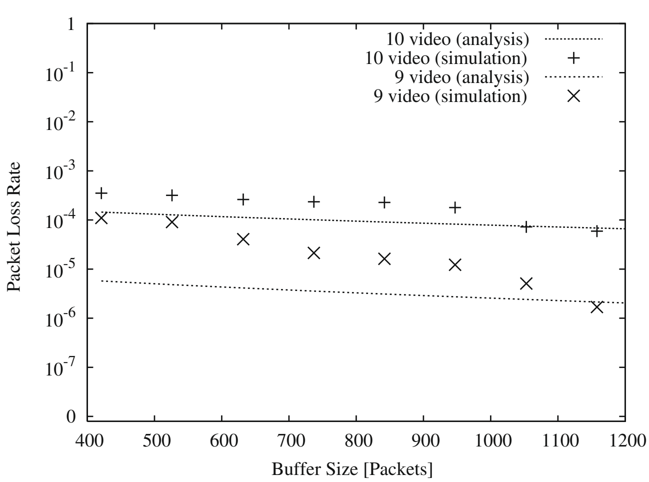


**Fig. 4.** Performance of video and CBR data in an 85 Mbps wired link.

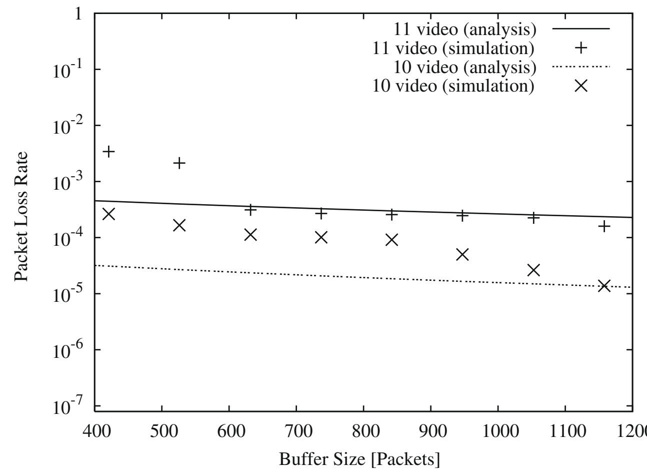


**Fig. 5.** Performance of video and On–Off data in an 85 Mbps wired link.

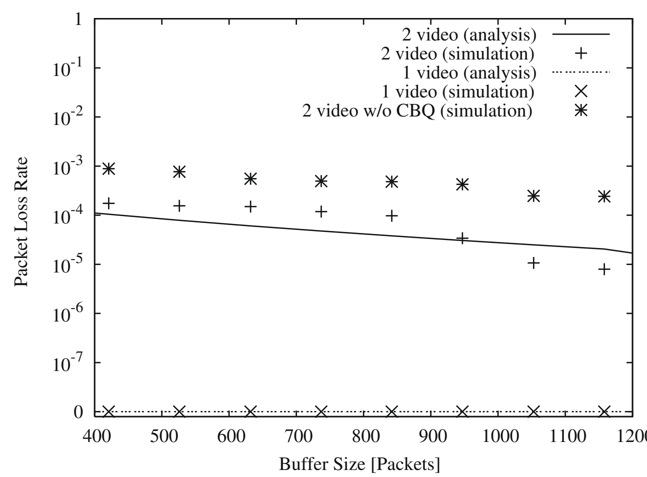


**Fig. 6.** Performance of video (with CBR data) in a 3-hop wireless path.

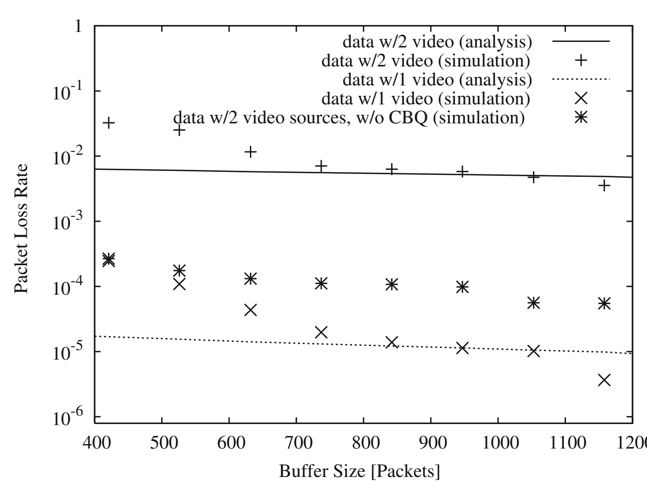


**Fig. 7.** Performance of CBR data (with video) in a 3-hop wireless path.

Since we use a log scale on the y-axis, the discrepancy is exaggerated. This discrepancy is mainly due to the limitation of the mini-source traffic model that does not consider the Group of Picture (GoP) structure of the MPEG codec. Since the mini-source model only considers the average traffic arrival rate of a GoP, the queue variation within a GoP is under-estimated. If we use more accurate traffic models, such as the model proposed in [20], the analytical results with a small buffer size will better match the simulation results. However, the computational complexity with the traffic model in [20] is much higher. On the other hand, as the QoS requirements of IPTV are stringent, we need to ensure that the packet loss rate is below $10^{-4}$–$10^{-6}$, so the buffer size needed is relatively large and the analytical results with the mini-source traffic model are accurate in this region. Therefore, the mini-source traffic model is appropriate for deriving the admission region in this paper.

During the simulation time, the number of packets generated is on the order of $10^7$, thus the achievable accuracy of the simulation is $10^{-7}$. The results below $10^{-7}$ appear as 0. The packet loss rate (PLR) constraint for HD format IPTV traffic is $10^{-5}$–$10^{-6}$ according to [12]. However, the PLR requirements in the standards for video over wireless networks are typically much looser and thus $10^{-4}$ is tolerable, e.g., with 3GPP [21]. To verify the analytical framework and limit the simulation time, $10^{-4}$ is chosen here as the PLR target.

In Fig. 4, both the analytical and simulation results show that, if one data source keeps transferring at a CBR of 5 Mbps, to ensure a PLR less than $10^{-4}$, a maximum of 10 IPTV connections can barely be supported with a buffer size larger than 1000 packets. Nine IPTV connections can be supported with a safe margin.

In a typical home network, data traffic tends to be more bursty than CBR. With typical bursty data traffic, Off periods can be up to 10 times an On period. Given the appropriate link-sharing mechanism, IPTV and data traffic can be efficiently distributed inside the home simultaneously. As shown in Fig. 5, an 85 Mbps wired link can support 10 IPTV connections and one On–Off data connection. Simulation results (not illustrated), also show that a buffer size of 11 packets is sufficient to guarantee the PLR of the data traffic is less than $10^{-4}$. To allow 11 IPTV connections in the link is not appropriate since the PLR is always above $10^{-4}$ even with a buffer size over 1100 packets.

We conclude that for an 85 Mbps wired link with CBQ, the admission region is 10 video sources in the presence of a 5 Mbps bursty data traffic source. In the worst case where the data traffic is a 5 Mbps CBR source, the admission region drops to nine IPTV connections.

#### 4.2.2. Wireless network

The performance of IPTV and CBR data traffic in a 3-hop wireless relay path is shown in Figs. 6 and 7, respectively. With 5% of the bandwidth reserved for data, it is impossible to support more than one IPTV connection. The PLR of the two traffic classes is up to $10^{-4}$ for video and $10^{-2}$ for data when two IPTV connections and one data connection are sharing the network.

To study the effect of CBQ on the admission region, we simulated the same scenario, omitting the use of CBQ. We noticed that the video performance is degraded, while at the same time, the PLR of the data source is lower (i.e., improved performance). This behavior is expected because CBQ is used to protect the IPTV traffic from the more aggressive data traffic.

When there is only one IPTV connection over the 3-hop wireless path, the quality of video is ensured, but the PLR of the data traffic is up to $10^{-4}$, as shown in Fig. 7. If we further increase the buffer size for data, the data PLR would be lower, but this may increase the queueing delay and jitter. Another means of lowering the data PLR involves increasing the reservation for data traffic using CBQ. For the 3-hop wireless path case, if 10% of the total bandwidth is reserved for data traffic, the PLRs for both the IPTV connection and the data connection are below $10^{-6}$. Therefore, if bandwidth is reserved appropriately, IPTV and data performance can be improved, and the QoS for both guaranteed.

Using appropriate resource management, video and data traffic can be supported over a multi-hop wireless path. Although the average throughput of each hop is 85 Mbps, the same as that of the wired link, the admission region for the 3-hop wireless network is only one-ninth that of the wired link. This is because, first, each packet must be transmitted in three time slots to avoid collisions; and second, the time variation of the wireless channel decreases the effective capacity compared to the wired link.

The admission regions of the IPTV traffic, accompanied by one data connection, are summarized in Table 1. It also gives the minimum buffer size needed to guarantee a PLR less than $10^{-4}$. For heterogeneous wireless and wired networks, the admission region is determined by the admission region of the bottleneck link. For the admission regions obtained over the 20 simulation runs, we count the number of runs with PLR above the threshold and obtain the confidence level of the admission region, as shown in Table 1.

#### 4.2.3. IPTV competing with TCP

We next investigate IPTV competing with TCP traffic. If the aggregate video data rate is less than the bandwidth allocated to video, TCP can probe for available bandwidth, efficiently utilize it, and even create transient congestion, due to its adaptive congestion control algorithm. However, this aggressive behavior should not affect the IPTV QoS with the protection of CBQ [19].

First, we let IPTV and TCP data traffic share a bottleneck link of 85 Mbps without CBQ. With eight IPTV sources, the video PLR is up to $10^{-4}$ even with a 1000 packet buffer. The average throughput of TCP is quite high, around 44 Mbps, however, the instantaneous TCP throughput is highly variable, and sometimes drops to near zero.

Second, we separate the IPTV and TCP traffic by allocating dedicated bandwidth to each, e.g., 95% of the 85 Mbps link capacity is dedicated to IPTV traffic, and the remaining 5% to TCP traffic. In this case, if the PLR requirement is $10^{-5}$, we can support at most eight IPTV flows with a buffer size exceeding 800 packets, as shown in Fig. 8.

Next, we multiplex eight IPTV flows and a TCP flow in the 85 Mbps link with CBQ, and assign 95% of the link capacity to IPTV when congestion occurs. The results show that the PLR of eight IPTV connections is much lower than that in the previous case. The same conclusion is reached if we compare the loss rate of nine IPTV flows occupying dedicated bandwidth and that when sharing the link with TCP using CBQ.

Therefore, by multiplexing IPTV and TCP data traffic together appropriately using CBQ, the PLR of IPTV can be reduced, thus more

**Table 1**
Admission region of IPTV traffic.

| Link type | Data | Bandwidth allocated for data (%) | Admission region | | Buffer size (packets) | Confidence level (%) |
|---|---|---|---|---|---|---|
| | | | Analysis | Simulation | | |
| Wired | CBR | 5 | 9 | 9 | 400 | 95 |
| | On–Off | 5 | 10 | 10 | 400 | 90 |
| 3-hop wireless | CBR | 5 | 1 | 1 | 600 | 90 |
| | CBR | 10 | 1 | 1 | 400 | 100 |

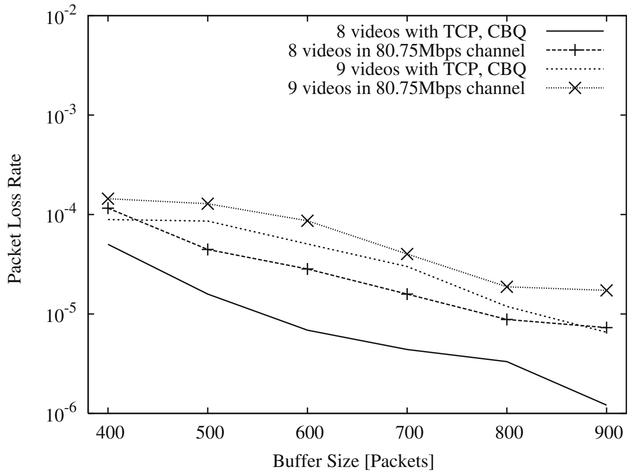


**Fig. 8.** Performance of video competing with TCP data.

IPTV flows can potentially be supported by taking advantage of the multiplexing gain.

## 5. Conclusions

In this paper, we have investigated the packet-loss performance of IPTV and data traffic over wired and multi-hop wireless paths. Given the link characteristics and IPTV and data traffic requirements, we have quantified the admission region for triple-play services in a wireless and wired network, with or without CBQ. Extensive simulation results have been obtained to validate the analysis. The simulation results also demonstrate the effectiveness of CBQ, as a resource management scheme, for deploying triple-play services in-home networks. The analytical framework presented here is adaptable to all traffic classes and link types. In addition, it can help service providers improve the design and deployment of home networks, and provide important insight into which system parameters affect the admission region of home networks.

## References

[1] S. Floyd, V. Jacobson, Link-sharing and resource management models for packet networks, IEEE/ACM Trans. Network. 3 (4) (1995) 365–386.
[2] B. Maglaris, D. Anastassiou, P. Sen, G. Karlsson, J. Robbins, Performance models of statistical multiplexing in packet video communications, IEEE Trans. Commun. 36 (7) (1988) 834–844.
[3] A.J. Laub, Matrix Analysis for Scientists and Engineers, SIAM Publications, Philadelphia, PA, 2005.
[4] P.T. Brady, A model for generating on–off speech patterns in two-way conversations, Bell Syst. Tech. J. 48 (1969) 2445–2472.
[5] L. Kleinrock, Queueing Systems Theory, vol. 1, Wiley, New York, 1975.
[6] M. Decina, T. Toniatti, On bandwidth allocation to bursty virtual connections in ATM networks, in: Proceedings of the IEEE International Conference on Communication, April 1990, pp. 844–851.
[7] The Network Simulator NS-2. Available from: <http://www.isi.edu/nsnam/ns>.
[8] P. Seeling, M. Reisslein, Evaluating multimedia networking mechanisms using video traces, IEEE Potentials 24 (4) (2005) 21–25.
[9] S. Deng, Empirical model of WWW document arrivals at access link, in: Proceedings of the IEEE International Conference on Communication, June 1996, pp. 1797–1802.
[10] IEEE Standard 802 Part 15.3: Wireless Medium Access Control (MAC) and Physical Layer (PHY) Specifications for High Rate Wireless Personal Area Networks (WPAN), 2003.
[11] L.X. Cai, L. Cai, X. Shen, J. Mark, Capacity of UWB networks supporting multimedia services, in: Proceedings of the QShine, August 2006.
[12] DSL Forum architecture & transport working group, Triple-play services quality of experience (QoE) requirements, in: DSL Forum, Technical Report TR-126, December 2006.
[13] D. Anick, D. Mitra, M.M. Sondhi, Stochastic theory of a data-handling system with multiple sources, Bell Syst. Tech. J. 61 (1982) 1871–1894.
[14] D. Mitra, Stochastic theory of a fluid model of producers and consumers coupled by a buffer, Adv. Appl. Probab. 20 (3) (1988) 646–676.
[15] J. Kim, M. Krunz, Bandwidth allocation in wireless networks with guaranteed packet-loss performance, IEEE Trans. Network. 8 (3) (2000) 337–349.
[16] E. Shihab, F. Wan, L. Cai, T.A. Gulliver, N. Tin, Performance analysis of IPTV in home networks, in: Proceedings of the IEEE Globecom, November/December 2007, pp. 5341–5345.
[17] A. Elwalid, D. Mitra, Analysis, approximations and admission control of a multi-service multiplexing system with priorities, in: Proceedings of the IEEE INFOCOM, April 1995, pp. 463–472.
[18] H.S. Wang, N. Moayeri, Finite-state Markov channel – a useful model for radio communication channels, IEEE Trans. Vehicular Technol. 44 (1995) 163–171.
[19] F. Wan, L. Cai, A. Gulliver, Can we multiplex IPTV and TCP? in: Proceedings of the IEEE International Conference on Communication, May 2008, pp. 5804–5808.
[20] F. Wan, L. Cai, A. Gulliver, A simple, two-level Markovian traffic model for IPTV video sources, in: Proceedings of the IEEE Globecom, November/December 2008, pp. 1–5.
[21] 3GPP TS 23.107 V 5.10.0 (2003-09), Technical Specification Group Services and Systems Aspects, Service Aspects; QoS concept and architecture (Release 5).